# Microstructure and mechanical properties of prototypic electron beam welds used to fabricate AISI 316L target vessels for the Spallation Neutron Source

Maxim Gussev, David McClintock, Donovan Leonard, Drew Winder

OAK RIDGE NATIONAL LABORATORY
MANAGED BY UT-BATTELLE FOR THE DEPARTMENT OF ENERGY

## Introduction

During operation, the tenth operational target module at the Spallation Neutron Source, referred to as Target 10, developed a leak at an electron beam (EB) weld used to join the front body and transition section of the mercury target vessel named EBW 3, as shown in Figure 1.

Though the exact cause of the Target 10 leak was not known, there were concerns that welding through the carbon atmosphere of a surface hardening treatment used to protect the target vessel, called Kolsterising® (K-layer), produced carbon-rich precipitates that might degrade the performance of the weld.

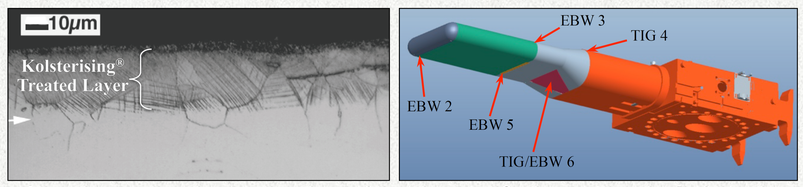


***Figure 1.*** *Cross-sectional view of Kolsterising® treated layer [left image from: Farrell and Byun, JNM, 356 (2006) 178-188] and diagram of welds used to fabricate SNS mercury target vessel.*

A testing campaign was initiated to characterize the condition of welds that are prototypical to those used to fabricate SNS target modules. Tensile and microstructural specimens were produced from weldments representing various weld conditions used to fabricate SNS target modules. The samples were characterized using tensile testing with digital image correlation, optic and electron microscopy.

## Experimental Procedures

SNS targets are fabricated using an electro-slag remelt (ESR) 316L steel. For the present work, the weldment mockups were fabricated from the ESR 316L plates used earlier to fabricate SNS targets. Eight weldment mockups were produced using single-pass EB welds, double-pass EB welds, and TIG over-weld repair welds.

Prior to welding, the K-layer was removed from sections of the plates by machining approximately 0.020 in of material from the top and bottom of the plates near the faying surfaces. After sections of the K-layer were removed, the weldment plates were tack welded together to secure the plates during welding, Figure 2. Weldment specimens (Figure 3) were fabricated using the same electron welder settings and geometry as the EBW 3 target weld.

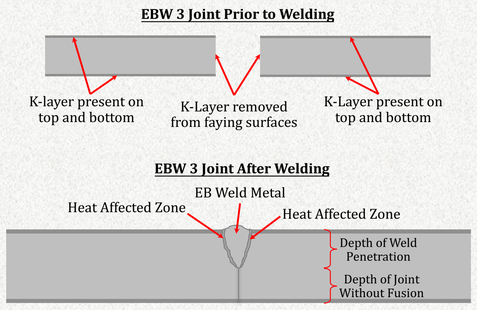


***Figure 2.*** *Illustration of weld preparation and configuration for EB welds.*

*Note: the thickness of K-layer and sections are not drawn to scale*

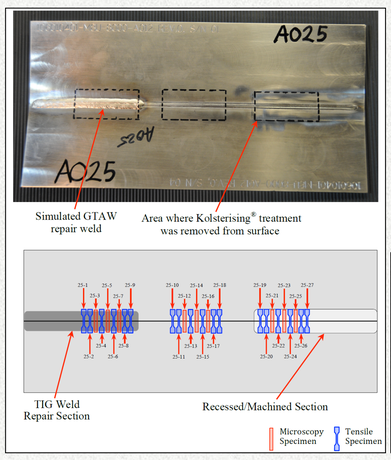


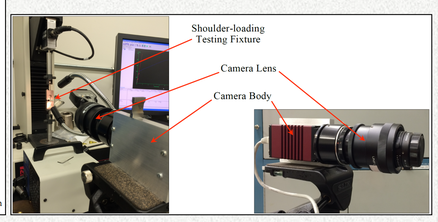


***Figure 3.*** *An image and specimen machining map for a typical mockup weldment (left) and DIC system setup (below).*

Tensile specimens of the SS-3 geometry were used; thickness, width, and length of gauge sections were 0.035 in, 0.060 in, and 0.300 in, respectively. Strain rate was ~$10^{-3}$ $s^{-1}$.

Tensile tests were recorded using a digital image correlation (DIC) system, Figure 3. The DIC system was used to measure the strain on various areas of the specimens and characterize any non-uniform deformation experienced by the weld region during deformation.

A JEOL JXA-8200X electron probe microanalyzer (EPMA) was used to examine the weld specimens for both microstructure and chemical composition. In addition to the microstructural analysis, both wavelength dispersive (WDS) and energy dispersive (EDS) X-ray analysis was performed.

## Results

### Kolsterising® Layer Evolution

One of the primary goals was to study the evolution of K-layer during the welding. A typical backscattered electron micrograph and X-ray maps of a region containing the boundaries between the weld, HAZ, and the non-affected K-layer are shown in Figure 4.

The carbon atmosphere of the K-layer is clearly visible in the carbon X-ray map on the right side of the image away from the weld in the base metal microstructure. Moving to the left from the base metal, the carbon content drops gradually to the background concentration level in the weld metal. It appears that K-layer is dissolved into solid solution; no carbon-rich precipitates were observed in the near-surface layer.

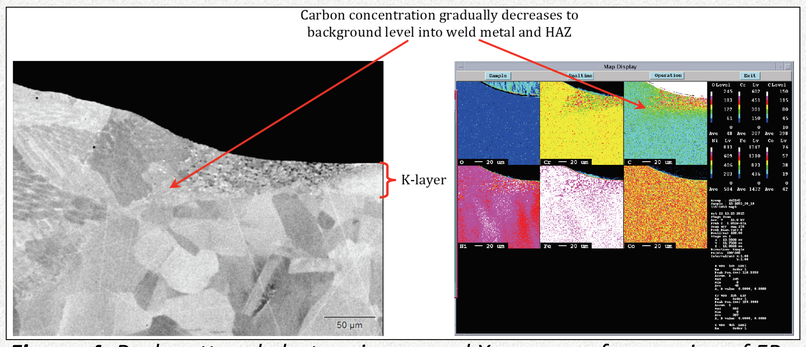


***Figure 4.*** *Backscattered electron image and X-ray maps for a region of EB-welded specimen containing the boundary between the HAZ and the non-affected K-layer, showing dissolution of carbon from the K-layer into the microstructure of the HAZ and weld metal.*

### Weldment Microstructure Analysis

The microstructures of specimens from each region of the weldments were characterized using an advanced electron microprobe, primarily to search for carbon-rich particles in the weld metal and heat affected zone (HAZ).

Shown in Fig. 5 is a composite of two micrographs of the specimen from single-pass EB weldment. This specimen was from a region with the K-layer present on the surfaces above and below the faying surfaces and provides a good representation of the general weld structure for all specimens. At the weld face, the grains in the weld metal are larger than the base metal grain size and have a columnar structure oriented normal to the weld face and the faying surfaces. No signs of carbon-rich precipitates caused by welding were reliably observed.

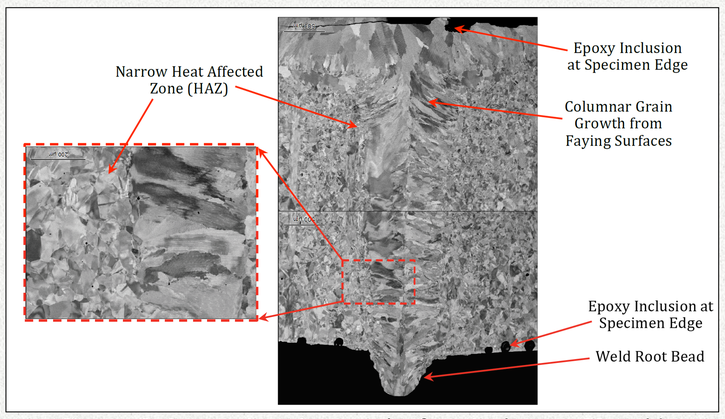


***Figure 5.*** *Composite micrograph after single-pass EB weld.*

### Weldment Mechanical Performance

All the specimens with a single-pass EB weld in the gauge section experienced some small increase in yield strength commensurate with an appreciable loss of ductility relative to the base metal, as shown in Figure 6.

Very little scatter was observed in the yield strength values, while appreciable scatter observed in the ultimate strength and elongation values. One of the scatter sources is likely the small specimen size, which contains a relatively small volume of the weld and the measured tensile properties are therefore susceptible to differences in the weld and grain structure. However, no cases of brittle fracture or fracture at small load/elongation values were observed suggesting the absence of internal cracks and other weld-related defects.

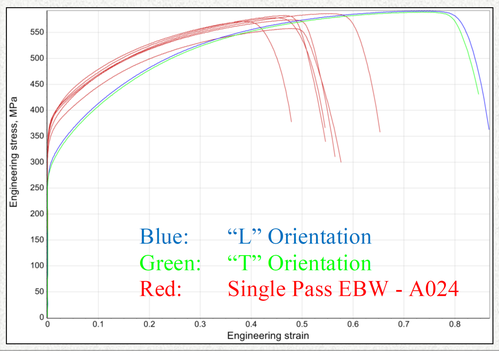


***Figure 6.*** *Engineering stress-strain curves for tensile specimens containing single-pass electron beam welds from weldments. T and L are base metal specimens (T: gauge length perpendicular to the weldment, L: parallel to the weldment).*

### Local Mechanical Behavior and Fracture

The DIC data was analyzed to characterize the deformation behavior, which displayed complex mechanical behavior. As a rule, several local strain maximums formed along the gauge and often competing necks were observed.

Test results for an EB-weld specimen is shown in Figure 7. Several small areas of concentrated strain existed at the beginning of the test (green curve), but the center of the gauge section (Point A) had the highest strain level. As the test progressed, the blue curve, the center location of localizing strain at point A continues to have the highest strain level, while four definite areas of localized strain begin to form in the gauge section. Near the end of the test, a switch in the dominant strain localization was made from point A to point B (red curve) and the specimen ultimately failed at point B. The competing necks are an indication that the tensile properties along the gauge section are similar, and no one region of the gauge section was significantly weaker or stronger than other regions.

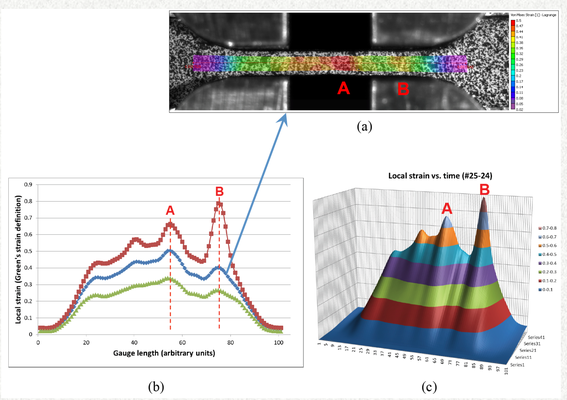


***Figure 7.*** *(a) Strain distribution map for EB-welded specimen at a point in the test corresponding to the blue strain curve in (b) the strain plots for the gauge section at different times of the test, and (c) a surface plot of the strain distribution along the gauge section for duration of the test.*

The fracture location appeared to be different for the specimens with and without the K-layer present on the top and bottom surfaces during welding, as shown in Figure 8. Specimens welded with the K-layer present often failed inside the weld region, while specimens with the K-layer removed frequently fractured outside the weld region.

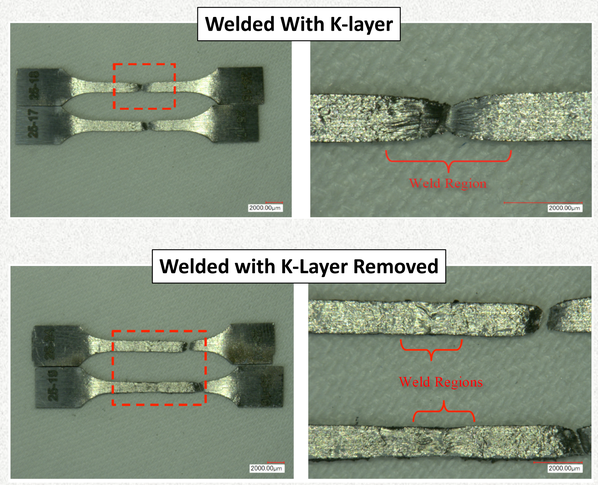


***Figure 8.*** *Tensile specimens after testing with K-layer present during welding (top) and with the K-layer removed before welding (bottom)*

## Conclusions

Carbon atmosphere of the hardened Kolsterising® layer (K-layer) appears to dissolve into solid solution during welding. Nonmetallic inclusions from the steel-making process were observed in the base and weld metal of specimens, but no large carbon-rich precipitates associated with the K-layer were found.

The tensile test results showed that the welded specimens experienced some increase in yield strength and decrease in ductility. The average yield strengths for the parent material were approximately 270 MPa, while the average values for the welded specimens were approximately 350 MPa, corresponding to an increase of ~25%. Engineering elongation values for welded specimens had considerably more scatter compared to the strength values, with total elongation values ranging from 50 to 60%. While ductility was reduced for all welded specimens relative to the base metal specimens, the elongation values measured for welded specimens are appreciable and are not a cause for concern.

The results of this testing campaign indicate that electron beam welding through the K-layer does not appreciably degrade the weld tensile strength, microstructure, or general performance.

The SNS is sponsored by the Office of Science, U.S. Department of Energy, and managed by UT-Battelle, LLC for the U.S. Department of Energy under Contract DE-AC05-00OR22725.

Research sponsored by Oak Ridge National Laboratory's Shared Research Equipment (ShaRE) User Program, which is sponsored by the Office of Basic Energy Sciences, U.S. Department of Energy.